Energy deposition at front and rear surfaces during picosecond laser interaction with fused silica

A. Salleo
Department of Materials Science and Engineering, University of California, Berkeley, Berkeley, California 94720 and Lawrence Livermore National Laboratory, Livermore, California 94550

F. Y. Génin,[a] M. D. Feit, and A. M. Rubenchik
National Ignition Facility, Lawrence Livermore National Laboratory, Livermore, California 94550

T. Sands
Department of Materials Science and Engineering, University of California, Berkeley, Berkeley, California 94720

S. S. Mao and R. E. Russo
Lawrence Berkeley National Laboratory, Berkeley, California 94720

(Received 12 December 2000; accepted for publication 13 February 2001)

The difference between front-surface and rear-surface energy deposition of a 35 ps laser pulse ($\lambda=1064$ nm) in fused silica was investigated using shadowgraphic and laser-deflection techniques. Shock waves were observed in the glass and in air. Shock waves generated in air at the front surface are stronger than at the rear surface. Less than 35% of the energy incident on the surface drives the air shock waves at the rear surface. Up to 90% of the incident energy drives the air shock waves at the front surface. Laser-plasma interaction is responsible for this difference and for limiting the amount of energy deposited inside the sample during front-surface ablation. Energy deposition at the rear surface is mostly limited by self-focusing inside the material. © *2001 American Institute of Physics.* [DOI: 10.1063/1.1362332]

Contrary to absorbing materials, energy deposition in transparent dielectrics cannot rely on intrinsic linear absorption. Energy absorption is due to impurities or imperfections[1,2] and is, therefore, nonuniform, unless the radiation intensity exceeds the intrinsic breakdown threshold of the material through nonlinear absorption.[3] Moreover, both the front and the rear surfaces of a sample as well as its bulk can couple to the electromagnetic field.[4–6] In the nanosecond regime, the interaction of the laser with the front surface of transparent dielectrics is very different than with the rear surface. Energy deposition causes more severe cracking and a higher removal rate per pulse at the rear surface.[7,8] This can be qualitatively explained by the deposition of energy inside the material at the rear surface and plasma shielding at the front surface. Also, material at the rear surface is more easily ejected because it is not capped by a plasma backpressure.[9] In this letter, we present a study of the interaction of 35 ps pulsed-laser radiation with both fused-silica surfaces.

In a first set of experiments, the fused-silica surfaces were imaged in cross section at short time delays after the pulse ($t<33$ ns). In a second set of experiments, the expansion rate of the laser-generated shock wave in air was measured at longer time delays ($t<10$ μs). The imaging experiments were performed using the fundamental frequency of a Nd:YAG Q-switched laser ($\tau=35$ ps and $\lambda=1064$ nm) as the pump beam. The second harmonic of the same laser output was used to illuminate the interaction region perpendicularly to the pump beam, and image it with different delays on a charge-coupled-device (CCD) camera equipped with a narrow-band 532 nm filter. The beam diameter was varied between 110 and 250 μm. A full description of the experimental system can be found elsewhere.[10] The experimental system used to measure shock-wave expansion was based on the deflection of a He–Ne laser beam by the shock-wave front, described in Fig. 1. The samples were 5.5 mm thick, 20 mm long, and 5 mm wide. All surfaces were polished. For all experiments, the laser fluence was significantly higher than the breakdown threshold of the studied surface (approximately 8 J/cm^2 at 35 ps in fused silica)[3] in order to ensure uniform and reproducible energy deposition within the center of the Gaussian beam and reduce the effect of surface defects.

Figure 2 is a set of shadow graphs of the shock waves in air and glass obtained at the rear surface 33 ns after 12.8, 20,

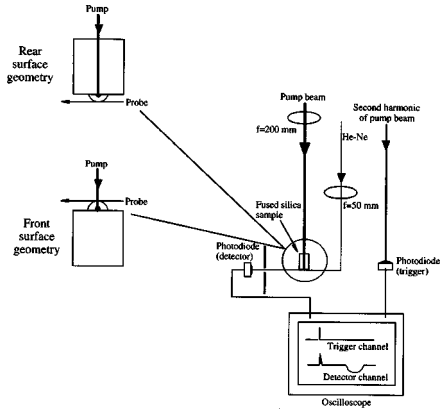

FIG. 1. Sketch of the laser-deflection setup with typical oscilloscope traces. The shock wave deflects the He–Ne beam and causes a dip in the trace of the detector channel.

[a]Author to whom correspondence should be addressed; electronic mail: fgenin@llnl.gov

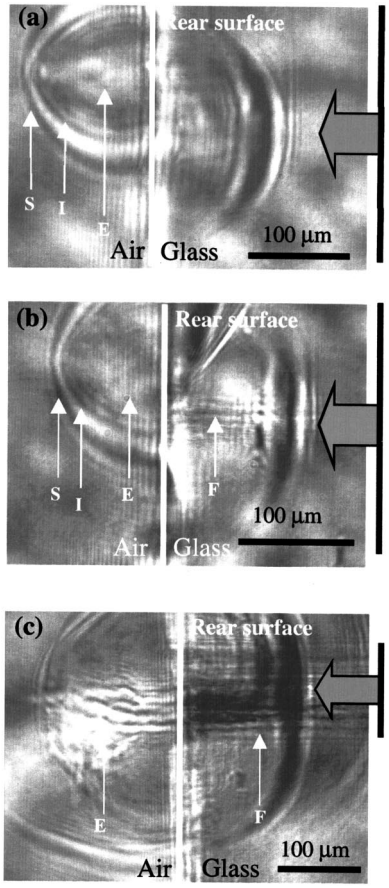

FIG. 2. Shadow-graphic images of shock waves generated in air and fused silica during rear-surface shots at 12.8 J/cm^2 (a), 20 J/cm^2 (b), and 280 J/cm^2 (c). The time delay is 33 ns. The features labeled in the figures are the shock front (S), the ionization front (I), and the ejected material (E). Filamentation (F) is also visible at higher fluences. The vertical black bar on the right of the images represents the $1/e^2$ diameter of the beam.

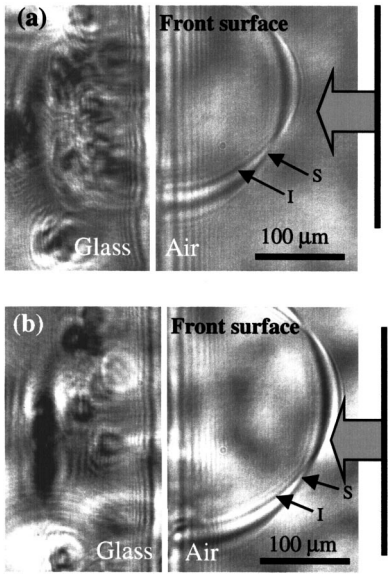

FIG. 3. Shadowgraphic images of shock waves generated in air and fused silica during front-surface shots at 14.4 J/cm^2 (a) and 25 J/cm^2 (b). The time delay is 33 ns. The shock front (S) and the ionization front (I) are labeled in the figures. The vertical black bar on the right of the images represents the $1/e^2$ diameter of the beam. The scattering centers in the glass seen in (a) and (b) are not in the plane of the pump beam. They remain visible before and after the pulse and are not related to damage during the pulse.

and 280 J/cm^2 pulses. The vertical offset between the image of the two waves is a refraction effect due to a slight tilt of the sample parallel to the probe beam. The shocks are generated in a 30–100-μm-diam (depending on beam fluence) area. Their front must, therefore, be initially planar. The front becomes spherical as the disturbance propagates. After 33 ns, the shock wave in air is hemispherical while the shock wave in glass is still quasiplanar at all fluences. The higher the fluence, the more extended the planar wave front of the glass shock (Fig. 2), hence, the stronger the shock. The shock waves do not generate cracks inside the glass. The planar shape of the wave front suggests that the stress state after 33 ns is mostly due to piston-like compression. No shear wave is thus observed. As the fluence is increased, evidence of self-trapping in the central part of the Gaussian beam becomes apparent as thin horizontal filaments terminating at the glass/air interface.

The structure of the shock waves in air can be interpreted using the analysis of Callies, Berger, and Hugel.[11] Shadowgraphic imaging of phase objects is sensitive to the second derivative of the refractive-index distribution.[12] Therefore, the shock front appears as a succession of three alternating bright and dark bands. In Figs. 2(a) and 2(b), the shock front is separated from the ionization front by a very thin layer of shocked air. The ionization front is separated from the next front (the contact front) by shocked and ionized air. Ionization of air occurs because the temperature behind the shock front (estimated from its velocity)[13] is approximately 6000 K. The shock pressure estimated by the same method is 500 atm. The faintly visible contact front delimits the expansion of the ejected silica. It is not spherically symmetric: the expansion has a component normal to the surface. At 280 J/cm^2, a highly directional jet of material flies from the rear surface [Fig. 2(c)]. The jet is formed by glowing particles. Part of a shock wave generated at earlier times is visible in the lower-left corner of the same figure. Jet-like material ejection seems to be the result of a more explosive energy relaxation mechanism due to the high density of deposited laser energy.

Figure 3 is a set of shadow graphs of front-side shock waves in air and glass at different time delays and fluences. The shock waves in air are spherical while the ones in glass are somewhat planar. The ionization front and the shock front merge at their furthest point giving rise to a different morphology than the one observed in the rear-surface shock: shocked air is immediately thermally ionized behind the tip of the shock front. Because of laser-plasma interactions these shock waves have significantly higher temperature and pressure (as estimated from their velocities): 9000 K and 750 atm.[13] The ionization front is ellipsoidal with its long axis perpendicular to the surface. Therefore, the temperature must be highest at the tip of the shock wave, which initially had the highest velocity. In Figs. 3(a) and 3(b), the gas within the shock wave is completely transparent and no ejected or evaporated material is visible.

Figure 4(a) illustrates that the radius R of the expanding shock wave is proportional to $t^{2/5}$, as predicted by Sedov's blast wave theory for a point explosion.[11,14,15] This scaling allows us to estimate the energy E_0 necessary to drive the shock wave: for a hemispherical blast wave in air, $R = (2.38E_0/\rho_0)^{1/5}t^{2/5}$, where ρ_0 is the density of unperturbed

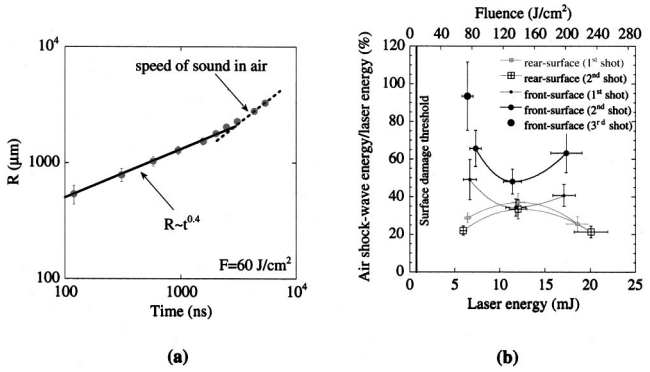

FIG. 4. (a) Rear-surface air shock-wave radius as a function of propagation time measured by laser deflection and (b) ratio of air shock-wave energy to laser energy on front and rear surfaces calculated using Sedov's formula. The third shot data point on the front surface follows a two-shot sequence at 200 J/cm^2. The curves are drawn only to guide the reader's eyes.

air.[16] Figure 4(b) is a plot of the ratio of the shock-wave energy to the beam energy as a function of beam energy. The fraction of beam energy expended in driving air shock waves on the rear surface is generally lower than on the front surface. For rear-surface shock waves, this fraction first increases with increasing fluence, indicating increased laser absorption at the surface. However, at 200 J/cm^2 the ratio decreases. This decrease is due to a combination of bulk damage (i.e., self-focusing filaments) and front-surface damage (a strongly absorbing plasma spark forms at the front surface when the fluence measured at the rear surface is higher than 150–170 J/cm^2). In the subsequent pulses, the amount of energy that reaches the rear surface for damage and shock-wave generation is progressively reduced. This explanation is consistent with the observation that shock-wave energy—hence, deposited energy—always decreases from the first to the second shot at the same location on the rear surface; the first shot always generated damage inside the bulk of the sample. Upon subsequent irradiation, laser drilling into the bulk was observed; systematic data on drilling rates were not recorded for this study.

The dependence of shock-wave energy on beam energy is the opposite at the front surface. This variation may be attributed to changes in the absorption coefficient of the front-surface plasma. The coefficient for bremsstrahlung absorption in an ionized plasma[17] is proportional to the product of ion and electron densities—until the plasma reaches critical density and is essentially opaque—and roughly proportional to $T^{-3/2}$. Therefore, colder plasmas (formed at lower fluence) and denser plasmas (formed at higher fluence) are more absorbing and drive stronger shocks. At constant fluence, a second shot always generates a stronger front-surface air shock than the first one, which indicates that the first shot increases surface absorption. After two shots at 200 J/cm^2, front-surface modifications cause nearly complete radiation absorption for all subsequent pulses. However, the study of front-surface ablation rates and crater morphology is beyond the scope of this letter and will be the subject of further investigation. Approximately 90% of the laser energy is dissipated in the shock after two high-fluence pulses. This fraction is in reasonable agreement with the results of Callies, Berger, and Hugel who reported that approximately 80% of the laser energy is expended in driving the shock wave during excimer laser ablation of copper.[11] The transmitted energy could not be measured directly because of the high intensity of the beam near the sample surface. Absorption at the front surface causes most of the laser energy to be deposited in air rather than being confined inside the sample. Therefore, less cracking and material removal are observed at the front surface as compared to the rear surface.[7,8,18]

A 35 ps, 1064 nm laser beam interacts differently with the front and rear surfaces of fused silica. This study shows that differences in the absorbed energy partition between air and silica are most probably responsible for this asymmetry. At the front surface, laser-plasma interactions during the pulse cause a large dissipation in the air, thus limiting the efficiency of energy deposition. At the rear surface the onset of front-surface absorption and self-focusing limit energy deposition. Energy is mostly confined inside the material when the beam interacts with the rear surface and dissipated in the air when the beam interacts with the front surface. Therefore, for a given absorbed energy, material removal efficiency is much higher at the rear surface than at the front surface.

This work was performed under the auspices of the U.S. Department of Energy by University of California Lawrence Livermore National Laboratory under Contract No. W-7405-Eng-48. Two of the authors (R.E.R. and S.S.M.) acknowledge support from the U.S. Department of Energy, Office of Basic Energy Sciences, Chemical Science Division, under Contract No. DE-AC03-76SF00098 at the Lawrence Berkeley National Laboratory. The authors wish to thank Dr. X. Mao and Dr. J. H. Yoo for their help and valuable discussions.

[1] C. Bandis, S. C. Langford, J. T. Dickinson, D. R. Ermer, and N. Itoh, J. Appl. Phys. **87**, 1522 (2000).
[2] J. T. Dickinson, J. J. Shin, and S. C. Langford, Appl. Surf. Sci. **96**, 316 (1996).
[3] B. C. Stuart, M. D. Feit, A. M. Rubenchik, B. W. Shore, and M. D. Perry, Phys. Rev. Lett. **74**, 2248 (1995).
[4] O. Yavas, E. L. Maddocks, M. R. Papantonakis, and R. F. Haglund, Appl. Phys. Lett. **71**, 1287 (1997).
[5] R. L. Webb, S. C. Langford, and J. T. Dickinson, J. Appl. Phys. **80**, 7057 (1996).
[6] J. Ihlemann, B. Wolff, and P. Simon, Appl. Phys. A: Solids Surf. **54**, 363 (1992).
[7] A. Salleo, T. Sands, and F. Y. Génin, Appl. Phys. A: Mater. Sci. Process. **71**, 601 (2000).
[8] A. Salleo, R. Chinsio, and F. Y. Génin, Proc. SPIE **3578**, 456 (1998).
[9] R. Kelly, A. Miotello, B. Braren, and C. E. Otis, Appl. Phys. Lett. **60**, 2980 (1992).
[10] S. S. Mao, X. L. Mao, R. Greif, and R. E. Russo, Appl. Phys. Lett. **76**, 31 (2000).
[11] G. Callies, P. Berger, and H. Hugel, J. Phys. D **28**, 794 (1995).
[12] W. Merzkirch, *Flow Visualization*, 2nd ed. (Academic, Orlando, FL, 1987).
[13] I. A. B. Zel'dovich and Iu. Raizer, *Physics of Shock Waves and High-Temperature Hydrodynamic Phenomena* (Academic, New York, 1966).
[14] L. I. Sedov, *Similarity and Dimensional Methods in Mechanics*, 10th ed. (CRC, Boca Raton, FL, 1993).
[15] M. Aden, E. W. Kreutz, H. Schluter, and K. Wissenbach, J. Phys. D **30**, 980 (1997).
[16] Z. Marton, P. Heszler, A. Mechler, B. Hopp, Z. Kantor, and Z. Bor, Appl. Phys. A: Mater. Sci. Process. **69**, S133 (1999).
[17] M. Von Allmen and A. Blatter, *Laser-Beam Interactions With Materials: Physical Principles and Applications*, 2nd updated ed. (Springer, Berlin, 1995).
[18] O. Yavas, E. L. Maddocks, M. R. Papantonakis, and R. F. Haglund, Appl. Surf. Sci. **129**, 26 (1998).